Electronic structure, optical properties, and bonding in alkaline-earth halofluoride scintillators: BaClF, BaBrF, and BaIF

N. Yedukondalu,[1] K. Ramesh Babu,[2] Ch. Bheemalingam,[1] David J. Singh,[3,*] G. Vaitheeswaran,[2,†] and V. Kanchana[4]

[1]*School of Physics, University of Hyderabad, Prof. C. R. Rao Road, Gachibowli, Hyderabad 500 046, Andhra Pradesh, India*

[2]*Advanced Centre of Research in High Energy Materials (ACRHEM), University of Hyderabad, Prof. C. R. Rao Road, Gachibowli, Hyderabad 500 046, Andhra Pradesh, India*

[3]*Materials Science and Technology Division and Center for Radiation Detection Materials and Systems, Oak Ridge National Laboratory, Oak Ridge, Tennessee 37831-6114, USA*

[4]*Department of Physics, Indian Institute of Technology Hyderabad, Ordnance Factory Estate, Yeddumailaram, 502 205, Andhra Pradesh, India*

(Received 8 December 2010; revised manuscript received 5 February 2011; published 15 April 2011)

We report first-principles studies of the structural, electronic, and optical properties of the alkaline-earth halofluorides, BaXF (X = Cl, Br, and I), including pressure dependence of structural properties. The band structures show clear separation of the halogen p derived valence bands into higher binding energy F and lower binding energy X derived manifolds reflecting the very high electronegativity of F relative to the other halogens. Implications of this for bonding and other properties are discussed. We find an anisotropic behavior of the structural parameters especially of BaIF under pressure. The optical properties on the other hand are almost isotropic, in spite of the anisotropic crystal structures.

DOI: 10.1103/PhysRevB.83.165117 PACS number(s): 78.20.Ci, 78.20.Bh

I. INTRODUCTION

Halides of simple metals would seem to be rather simple materials with ionic bonding, closed shell repulsions, and generally high band gaps. Nonetheless, they display a remarkably rich structural chemistry and a wide variety of interesting and useful properties.[1] These include their use as optical materials and as scintillators for high-energy physics, medical imaging, and other applications involving detection and spectroscopy of ionizing radiation.[2]

The alkaline-earth halofluorides MXF (M = Ca, Sr, and Ba; X = Cl, Br, and I) belong to the class of ionic materials crystallizing in the primitive tetragonal PbClF-type (space group 129, $P4/nmm$) Matlockite structure. This is a quasi-2D layered structure.[3–6] When activated with Eu, Sm, or Pr they display strong photostimulated luminescence (PSL). Based on this they have been used as image storing phosphors in x-ray systems, especially where accurate determinations of x-ray dose are needed.[7–10] In addition, the luminescence of these materials is a useful pressure gauge in high-pressure experiments.[11,12] Finally, there have been a number of studies of the structural, vibrational, and high-pressure properties of these materials.[13–26] They show anisotropic compressibilities and interesting composition dependent phase transitions, including a transition to a monoclinic ($P2_1/m$) phase in BaClF at 22 GPa. Returning to the response to ionizing radiation, the behavior of these halofluorides is in sharp contrast to apparently closely related materials, such as BaF_2 and BaIBr. In scintillators, ionizing radiation produces excitations, normally electron-hole pairs. These recombine radiatively at scintillation centers to produce light that is detected externally. Transport of energy in the form of electron-hole pairs to the scintillation centers is a key process.

BaF_2 has been applied as a scintillator both in pure and activated form.[27,28] Pure cubic BaF_2 is among the fastest scintillators, in the sense that most of the light output occurs within a very short time, ~0.8 ns, of the absorption (there is also a slower component that can be partially suppressed by La doping). BaIBr is a very high light output scintillator when activated with Eu.[29] Thus there is an efficient energy transfer in these materials. In contrast, the energy deposited by ionizing radiation in the Ba halofluorides is not efficiently transferred to the scintillation centers and instead there is a large PSL representing photoinduced release of trapped carriers. Here we present first-principles calculations of the electronic structure and optical, structural, and other properties and discuss the results in relation to the differences in properties from other halides. We find that the high electronegativity of F as compared to other halogen atoms plays an important role.

II. STRUCTURE AND COMPUTATIONAL METHODS

The density functional calculations presented here were done using two methods. The ambient pressure electronic structure and optical properties were obtained using the linearized augmented plane wave (LAPW) method.[30] This is an all electron full potential method. These calculations were performed using the WIEN2k package.[31] We used LAPW sphere radii of 2.65, 2.70, 2.65, 2.55, and 2.30 bohrs, for Ba, I, Br, Cl, and F, respectively. We employed well converged zone samplings and basis sets including local orbitals for the semicore states of Ba and to relax linearization errors.[32] Relativity was treated at the scalar relativistic level. We used the experimental lattice parameters[33–35] and relaxed the internal coordinates using the generalized gradient approximation (GGA) of Perdew, Burke, and Ernzerhof (PBE).[36] As mentioned, these compounds form in the tetragonal $P4/nmm$ PbClF structure, as depicted in Fig. 1. As may be seen, this is a layered structure, both from the point of view of the halogens and the Ba. The lattice parameters and calculated internal coordinates used in the LAPW calculations are given in Table I. The internal coordinates are very close to the experimental

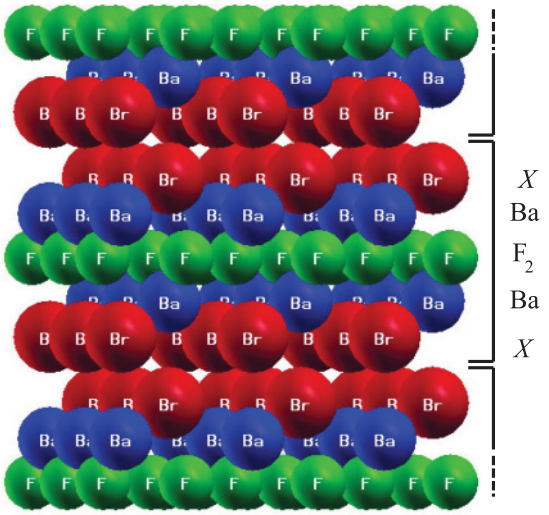

FIG. 1. (Color online) Crystal structure of the BaBrF using the calculated internal coordinates, showing the XBaF$_2$BaX layers. Note the weak Br-Br connections between these layers.

values and the results of the plane wave calculations for all three compounds, as shown in Table II.

As mentioned, we used the structures of Table I to calculate electronic and optical properties. However, standard density functionals are designed to reproduce the total energy as well as possible, but generally do not reproduce band gaps, and instead seriously underestimate the gaps of simple insulators, such as those considered here. For this we used the recently developed functional of Tran and Blaha, which we denote TB-mBJ.[37] This functional, which includes the kinetic energy density, greatly improves upon band gaps of semiconductors and insulators, including halides similar to the BaXF compounds discussed here.[37–39]

For the calculations of elastic constants and pressure dependent properties it was more convenient to use a plane wave basis. For this we used the CASTEP package.[40,41] The calculations were done using Vanderbilt-type ultrasoft pseudopotentials[42] with the local density approximation (LDA) as parametrized by Perdew and Zunger.[43] These are standard widely used LDA pseudopotentials. We verified convergence with respect to the plane wave cutoff and zone sampling. The calculations shown are for basis set cutoffs of 410 eV and $8 \times 8 \times 6$, $8 \times 8 \times 5$, and $5 \times 5 \times 3$ **k**-point sets, for BaClF, BaBrF, and BaIF, respectively. We used a criterion for self-consistency that the energy is converged to 5×10^{-7} eV/atom and the force to 10^{-4} eV/Å.

TABLE I. Structural parameters used in the LAPW calculations. The lattice parameters are from experimental data, while the internal coordinates are from total energy minimization using the LAPW method with the PBE GGA. The atomic coordinates are Ba at (1/4,1/4,v), X at (1/4,1/4,u), and F at (1/4,3/4,0) The experimental data for the lattice parameters are from Refs. 33, 34, and 35, for X = Cl, Br, and I, respectively.

	a (Å)	c (Å)	v	u
BaClF	4.3964	7.2315	0.2063	0.6466
BaBrF	4.503	7.435	0.1934	0.6471
BaIF	4.654	7.962	0.1720	0.6483

TABLE II. Lattice parameters a and c (in Å), and internal coordinates u and v. These are from plane wave calculations (LDA) and are compared with experimental data. Note the small differences from the LAPW calculations.

Compound	Quantity	LDA	Experiment
BaClF	a	4.281	4.3940 [20], 4.3964 [33]
	c	7.003	7.2250 [20], 7.2315 [33]
	u	0.6470	0.6472 [20], 0.6466 [33]
	v	0.2037	0.2049 [20], 0.2063 [33]
BaBrF	a	4.400	4.5080 [20], 4.5030 [34]
	c	7.210	7.4410 [20], 7.4350 [34]
	u	0.6480	0.6497 [20], 0.6483 [34]
	v	0.1900	0.1911 [20], 0.1934 [34]
BaIF	a	4.546	4.6540 [20], 4.6540 [35]
	c	7.678	7.9620 [20], 7.9620 [35]
	u	0.6484	0.6522 [20], 0.6483 [35]
	v	0.1689	0.1704 [20], 0.1720 [35]

Finally, we note that three different functionals are being used in the present calculations. These include the TB-mBJ functional, which is essential for the optical calculations because of the role that the band gaps play in optical properties. Unfortunately, the TB-mBJ functional cannot be used for total energies or structural properties.[37] Therefore to obtain the best possible electronic structure we use the experimental lattice parameters. These are known to a very high precision from diffraction. The internal coordinates are then determined using the PBE GGA fixing these lattice parameters and then obtaining the TB-mBJ electronic structure based on this structure. Turning to the pressure dependence we note that the LDA functional is known to underestimate lattice parameters. Standard GGA functionals, including PBE, have the opposite problem for heavy-element compounds such as those being studied here, and generally overestimate lattice parameters of such materials.[44,45] Also, standard GGA functionals lack binding for materials where dispersion interactions are important, such as graphite.[46] Considering this we used LDA calculations for the pressure dependent properties.

In order to characterize the differences between the LDA and PBE GGA for these compounds we did LAPW calculations for the structure of the middle compound, BaBrF, using both functionals. With the LDA we obtain $a = 4.41$ Å, $c = 7.24$ Å, $u = 0.6493$, and $v = 0.1923$ in good accord with our LDA plane wave pseudopotential calculations. With the PBE-GGA, we obtain $a = 4.57$ Å, $c = 7.58$ Å, $u = 0.6487$, and $v = 0.1906$. As expected the PBE-GGA lattice parameters are overestimated. Also, unlike the LDA, the PBE-GGA predicts c/a larger than experiment, consistent with underestimation of the interaction between the XBaF$_2$BaX blocks comprising the structure.

III. ELECTRONIC STRUCTURE

We begin with the electronic structure under ambient conditions, discussing the results obtained with the TB-mBJ functional. The band structures of BaClF, BaBrF, and BaIF, as

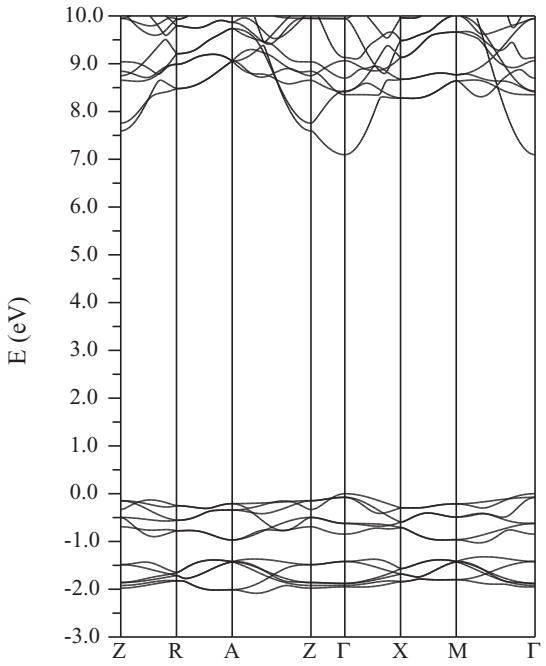

FIG. 2. Calculated band structure of BaClF using the TB-mBJ functional.

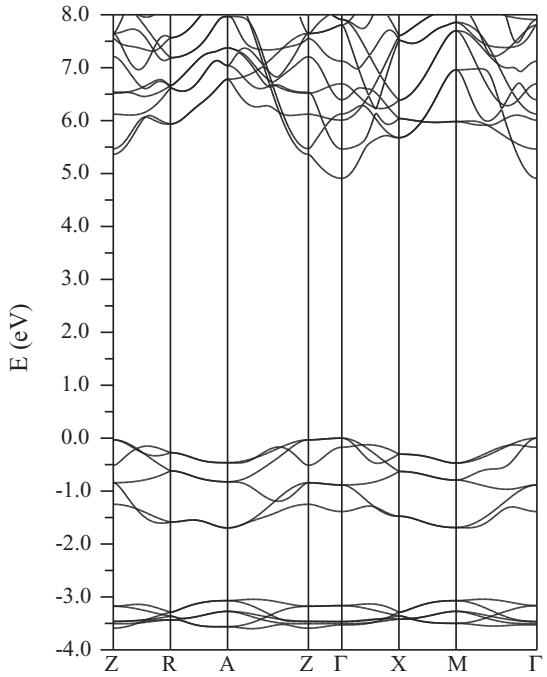

FIG. 4. Calculated band structure of BaIF using the TB-mBJ functional.

obtained with the TB-mBJ functional, are shown in Figs. 2, 3, and 4, respectively. The calculated TB-mBJ band gaps are 7.10 eV, 6.20 eV, and 4.91 eV for BaClF, BaBrF, and BaIF, respectively. The corresponding values with the PBE GGA are 5.41 eV, 4.82 eV, and 3.92 eV. We are not aware of optical spectroscopic measurements of the gaps with which to compare.

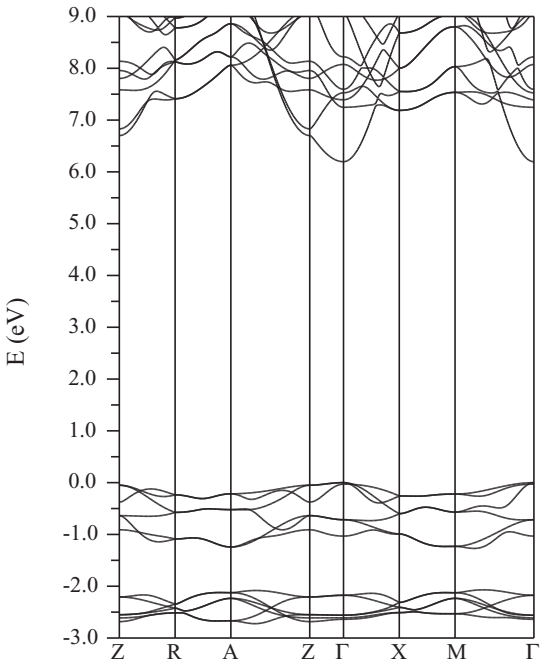

FIG. 3. Calculated band structure of BaBrF using the TB-mBJ functional.

The band structures show an important difference from the alkaline-earth halides containing mixtures of heavier halogens, such as BaIBr.[38] In particular, the valence bands are split into two distinct narrow manifolds: a lower manifold derived almost entirely from F $2p$ states and an upper manifold extending to the valence band edge derived from the p states of the other halogen. This was noted previously in the case of BaClF by El haj Hassan and co-workers,[25] although the splitting that we obtain for this compound with the TB-mBJ functional is larger. In all three compounds the distance from the top of the lower lying F derived manifold to the bottom of the conduction bands is close to 8.5 eV. This is $\sim$1 eV lower than the band gap of 9.77 eV obtained using the same method for cubic BaF_2. The position of the upper manifold follows the expected trend with electronegativity, showing a decreasing band gap as the atomic number increases and the electronegativity decreases. The reason why the two manifolds are cleanly separated here, but not in, e.g., BaIBr, is that the electronegativity difference between F (Pauling scale, 3.98) and the other halogens (3.16, 2.96, and 2.66 for Cl, Br, and I, respectively) is large and the $2p$ orbital of F is rather contracted compared to the other halogens. This is a consequence of the fact that the $2p$ orbital is the lowest orbital for that angular momentum and is reflected in the high electronegativity and small ionic radius of F. The Shannon radii of the halogen anions (sixfold coordination) are 1.19, 1.67, 1.82, and 2.06 Å for F^-, Cl^-, Br^-, and I^-, respectively. This results in reduced hopping and narrower F p bands and reduced hybridization between F $2p$ and the p orbitals of the other halogen. Importantly, this difference provides a way of explaining the different response of these materials to ionizing radiation, where activated BaIBr is a high light output scintillator,[29] while the BaXF are storage phosphors.

Ionizing radiation produces electron-hole pairs that recombine radiatively at a scintillation center in scintillators. A key step is the transfer of energy mainly in electron-hole pairs to the scintillation site. In a halide the holes exist in the halogen p derived valence bands, while the electrons are in metal derived conduction bands. As mentioned, the structure of the BaXF compounds consists of ionically bonded XBaF_2BaX layers (see Fig. 1) that are overall neutral and weakly joined to each other. Because the highest valence bands are derived almost entirely from the $X\,p$ orbitals, holes will be located on the X ions. Since these are anions, and holes are positively charged, the tendency will be for holes to exist on the parts of the X atoms facing toward the region between the XBaF_2BaX layers, i.e., in the X-X parts of the unit cell. Since the layers are weakly bonded to each other this is a favorable situation for hole self-trapping. Such self-trapped holes would be expected to have a very low probability of radiatively recombining with electrons associated with orbitals on the Ba ions, thus providing a plausible explanation for the different behavior of these compounds from scintillators such as BaIBr.

IV. STRUCTURE, ELASTIC CONSTANTS, AND PRESSURE DEPENDENCE

We calculated structural properties, elastic constants, and pressure dependence of the structure within the LDA using a plane wave method. The ambient pressure structural parameters are given in Table II. As may be seen, these are in good accord with existing experimental data, with the exception that as usual the LDA underestimates lattice constants by ~3%. The c/a ratios are underestimated relative to experiment, reflecting a larger underestimate of the c-axis lattice parameters than the a-axis lattice parameters. This reflects the relatively poor density functional description of the weak dispersion (van der Waals) interactions that are no doubt of importance in the interlayer X-X bonds.[47]

The elastic properties include elastic constants, Young's modulus, bulk modulus, shear modulus, and Poisson's ratio. These provide information about the mechanical stability and stiffness of materials under applied stress. There is also a link between the mechanical and dynamical behavior of solids as the elastic constants determine the slopes of the acoustic phonon branches near the zone center. We calculated the elastic constants for BaXF (X = Cl, Br, I) compounds within the LDA. Due to the tetragonal symmetry, these compounds have six independent elastic constants: C_{11}, C_{33}, C_{44}, C_{66}, C_{12}, and C_{13}. To calculate the elastic constants we used the volume conserving strains technique.[48] The calculated elastic constants are given in Table III. They are roughly ~25% larger than the reported experimental values. This is as expected for elastic constants calculated for the LDA equilibrium volume (a 7%–8% underestimate of the volume combined with a dimensionless pressure derivative of a modulus of 4–5, as is typical, implies overestimates of roughly this magnitude). The trends in the experimental data are, however, well reproduced. A key point is that all the materials are substantially anisotropic from an elastic point of view, for example C_{33} is smaller than C_{11}, C_{12} is smaller than C_{13}, and C_{44} is smaller than C_{66} in all cases, consistent with the structural picture discussed above, i.e., ionic XBaF_2BaX layers, stacked along c, and with relatively weaker interlayer bonding as compared to the intralayer bonding.

TABLE III. Calculated LDA elastic constants and Voigt bulk modulus B_V in GPa of the BaXF compounds in comparison with experimental data. The calculations were at the LDA equilibrium lattice parameters.

		C_{11}	C_{33}	C_{44}	C_{66}	C_{12}	C_{13}	B_V
BaClF	LDA	88.8	77.8	28.2	29.1	36.2	43.2	55.6
	Ref. 20							45
	Refs. 49, 50	71.9	65.6	20.4	23.8	28.2	31.9	43.7
BaBrF	LDA	80.5	65.1	23.6	30.3	34.9	41.8	51.5
	Ref. 20							42
	Ref. 49	71.3	55.4	20.9	24.7	25.0	34.3	42.8
BaIF	LDA	68.9	43.2	26.8	30.1	31.2	32.4	41.4
	Ref. 20							36
	Ref. 49	55.8	31.9	19.2	24.3		23.5	

The mechanical stability condition, which reflects the structural stability of materials, is important. The criterion for a elastically stable lattice is that the energy is a positive definite quadratic function of strain at small strain.[51] For these compounds we find that all the elastic constants are positive and obey the Born criteria for mechanical stability of tetragonal crystals: $C_{11} > 0$, $C_{33} > 0$, $C_{44} > 0$, $C_{66} > 0$, $(C_{11} - C_{12}) > 0$, $(C_{11} + C_{33} - 2C_{13}) > 0$, and $[2(C_{11} + C_{12}) + C_{33} + 4C_{13}] > 0$. The calculated elastic constants allow us to obtain the macroscopic mechanical properties of these compounds in bulk polycrystalline form, namely bulk modulus B and shear moduli G via two approximations, Voigt (V) and Reuss (R), as given by

$$B_V = \tfrac{1}{9}[2(C_{11} + C_{12}) + C_{33} + 4C_{13}], \quad (1)$$

$$G_V = \tfrac{1}{30}(L + 3C_{11} - 3C_{12} + 12C_{44} + 6C_{66}), \quad (2)$$

$$B_R = \frac{C^2}{L}, \quad (3)$$

$$G_R = 15\left[18\frac{B_V}{C^2} + \frac{6}{(C_{11} - C_{12})} + \frac{6}{C_{44}} + \frac{3}{C_{66}}\right]^{-1}, \quad (4)$$

with $L = C_{11} + C_{12} + 2C_{33} - 4C_{13}$ and $C^2 = (C_{11} + C_{12})C_{33} - 2C_{13}^2$.

We used the calculated C_{ij} to obtain the polycrystalline aggregate properties: the bulk modulus B, which measures the resistance of a material against volume change under hydrostatic pressure, and shear modulus G, which represents the resistance to shape change caused by shearing force in terms of the Voigt-Reuss-Hill approach.[52] In this approach, the Voigt and Reuss averages are taken as limits and the actual effective moduli for polycrystals can be approximated by the arithmetic mean of these two limits. Then one can calculate the average compressibility ($\beta_{\mathrm{VRH}} = 1/B_{\mathrm{VRH}}$), Young's modulus [$Y_{\mathrm{VRH}} = 9G_{\mathrm{VRH}}B_{\mathrm{VRH}}/(3B_{\mathrm{VRH}} + G_{\mathrm{VRH}})$], which reflects the resistance of a material against uniaxial tensions, and Poisson's ratio $\sigma = (1/2)\{[B_{\mathrm{VRH}} - (2/3)G_{\mathrm{VRH}}]/[B_{\mathrm{VRH}} + (1/3)G_{\mathrm{VRH}}]\}$, which generally provides an indication of the stability of the crystal against shear. The results are in Table IV. According to Pugh's criterion[53] a value B/G of 1.75 separates brittle from ductile materials. The calculated values for BaClF,

TABLE IV. Compressibility β (GPa^{-1}), shear modulus G (GPa), Young's modulus Y (GPa), and Poisson's ratio σ from the calculated LDA elastic constants.

Compound	β	G	Y	σ
BaClF	0.0179	25.5	66.5	0.30
BaBrF	0.0194	21.8	57.3	0.31
BaIF	0.0246	20.4	52.3	0.29

BaBrF, and BaIF are 2.19, 2.36, and 1.99, respectively, consistent with ductile behavior as expected for such ionic compounds.

Finally, we turn to the pressure dependent structural parameters as obtained within the LDA. The calculated structural parameters as a function of pressure are given in Figs. 5, 6, and 7 for BaClF, BaBrF, and BaIF, respectively. Our results for the pressure dependence of the structure of BaClF are similar to the LDA calculations reported by D'Anna and co-workers.[26] While the pressure scale is shifted between experiment and the LDA calculations reflecting the LDA underestimate of the equilibrium volume, the curves are otherwise in generally good agreement. One notable exception is that for BaBrF there is a hardening of the lattice seen in the experimental data in the range of ~10–20 GPa that is not present in the calculations. This is evident from the deviation of the experimental volume above the trend given by the LDA volume vs pressure in Fig. 6. While this may reflect limitations of the LDA, it would be very desirable to repeat the experiment for BaBrF in this pressure range. An important point is that the c/a ratio decreases with pressure for all three compounds over the pressure range studied. This is a continuation of the ambient pressure elastic anisotropy discussed above to high pressure, and again reflects the structural anisotropy of these compounds. This in turn is associated with the weak X-X connections between the layers, which have also been discussed in relation to high-pressure phase transitions in BaClF. [19] Finally, in relation to the next section, we emphasize that the density functional calculations do capture the anisotropy of the materials that is present in the experimental data.

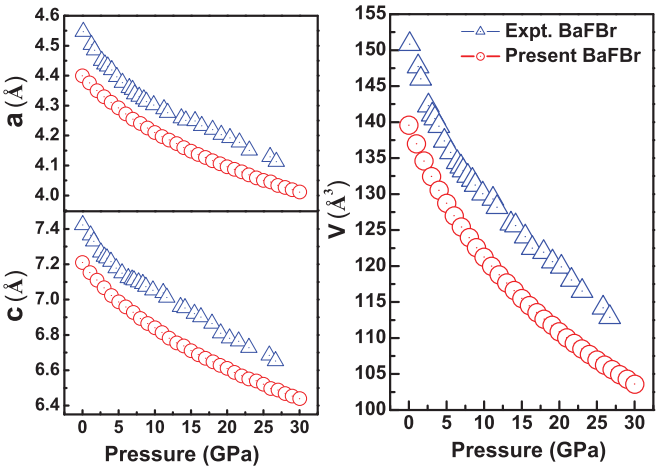

FIG. 6. (Color online) Pressure dependence of LDA structural parameters in comparison with experiment (Ref. 20) for BaBrF.

V. OPTICAL PROPERTIES

As mentioned, the structure of BaXF consists of XBaF$_2$BaX layers that are weakly bonded to each other. This is therefore a very anisotropic material from a structural point of view. Prior calculations for halide scintillators based on the heavy halogens showed that these materials show relatively little optical anisotropy even in cases where the crystal structures are very structurally anisotropic.[38,54]

We calculated the optical properties of BaClF, BaBrF, and BaIF, using the LAPW electronic structures that were obtained with the TB-mBJ functional. The calculated optical refractive indices of the three compounds are shown in Fig. 8. The usual trend toward higher refractive index with lower band gap is followed going from $X = $ Cl to $X = $ Br to $X = $ I. The calculated zero energy ($\lambda = \infty$) direction averaged refractive indices are 1.62, 1.71, and 1.85 for X = Cl, Br, and I. The differences between the c and a refractive indices are 0.3%, 0.8%, and 1.5% for the three compounds, respectively. These are at the level of the computational uncertainty. In any case, as may be seen, the trend toward weak optical anisotropy in heavy

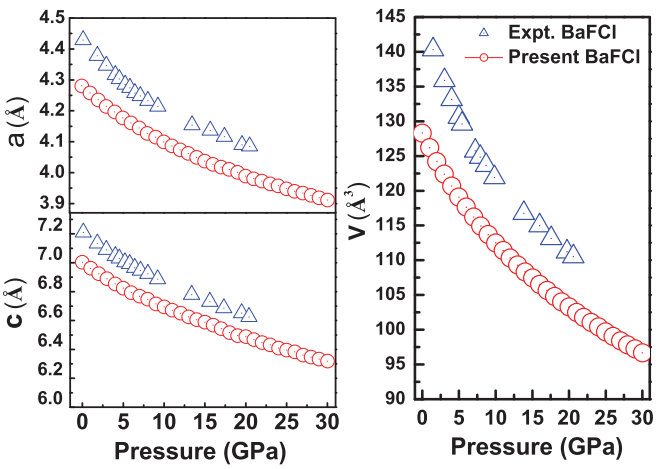

FIG. 5. (Color online) Pressure dependence of LDA structural parameters in comparison with experiment (Ref. 20) for BaClF.

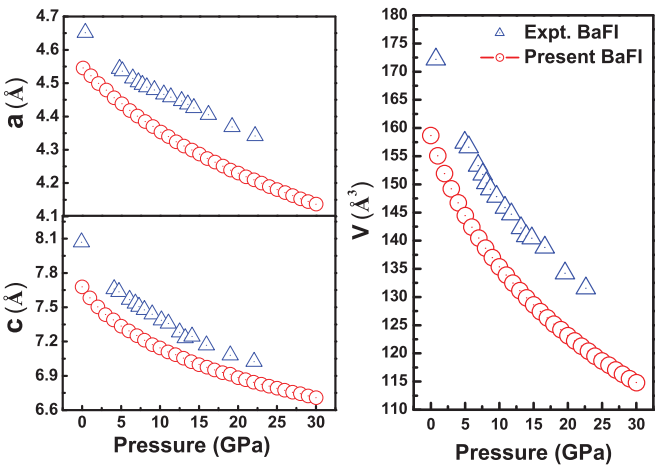

FIG. 7. (Color online) Pressure dependence of LDA structural parameters in comparison with experiment (Ref. 20) for BaIF.

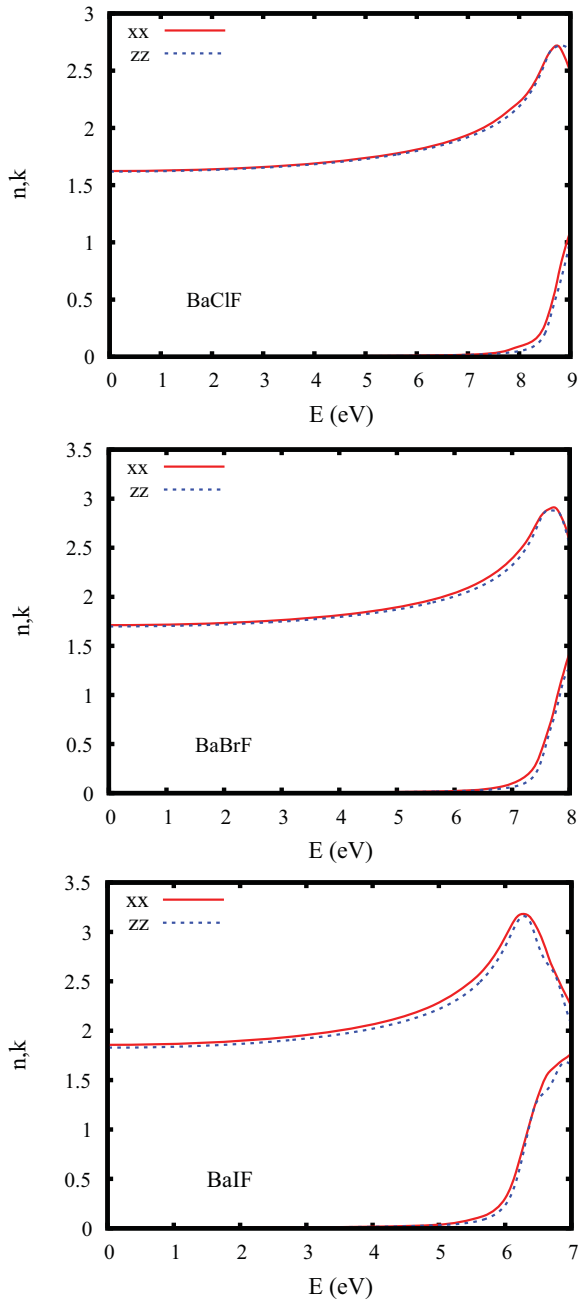

FIG. 8. (Color online) Calculated optical refractive index of BaClF (top), BaBrF (middle), and BaIF (bottom) as obtained with the TB-mBJ functional.

halides extends to the BaXF compounds, and in particular the optical anisotropy is very weak.

Therefore, in spite of the strong anisotropy of the structure, the elastic properties, and the pressure dependence, we find nearly isotropic optical properties. This should be favorable for the production of transparent ceramic storage phosphors based on these materials in analogy with transparent ceramic scintillators.[55] Previously, based on calculations similar to those presented here, we found that orthorhombic SrI_2 has very low optical anisotropy and should therefore be amenable to fabrication as a transparent ceramic scintillator.[54] This was very recently confirmed by experiments demonstrating a translucent Eu^{2+} activated SrI_2 ceramic scintillator with high light yield, highly proportional response, and improved afterglow and lifetime as compared to single crystals.[56]

VI. SUMMARY AND CONCLUSIONS

We performed density functional calculations of the electronic, optical, elastic, and pressure dependent structural properties of BaClF, BaBrF, and BaIF. The valence bands show a separation into two manifolds: lower lying F derived bands and higher lying X (Cl, Br, I) bands. This is associated with the large electronegativity difference between F and the heavier halogens. In any case, it provides a plausible explanation of the different response to ionizing radiation seen in these compounds as compared to non-F-containing mixed halide scintillators. Essentially, this separation confines holes to the X layers where they may be subject to self-trapping.

The structural, elastic, and pressure dependencies of the structure all point to a strong anisotropy of these compounds reflecting $X\mathrm{BaF_2Ba}X$ ionic layers that are stacked along c and relatively weakly bound to each other. Nonetheless, we find that the optical properties of these compounds are very isotropic. This has implications for the possible use of these materials in transparent ceramic form.

ACKNOWLEDGMENTS

N.Y.K. thanks Professor C. S. Sunandana for valuable suggestions and a critical reading of the manuscript. N.Y.K. thanks the University of Hyderabad and AICTE for financial support, and the CMSD, University of Hyderabad, for providing computational facilities. K.R.B. thanks the DRDO through ACRHEM for financial support. Work at ORNL was supported by the Department of Energy, Nonproliferation and Verification Research and Development, NA-22.

*singhdj@ornl.gov
†gvsp@uohyd.ernet.in

[1]L. Pauling, *The Nature of the Chemical Bond and the Structure of Molecules and Crystals: An Introduction to Modern Structural Chemistry*, 3rd ed. (Cornell University Press, Ithaca, 1960).
[2]G. Knoll, *Radiation Detection and Measurement*, 3rd ed. (Wiley, New York, 2000).
[3]F. Hulliger, *Structural Chemistry of Layer Type Phases* (Reidel, Dordecht, 1975), p. 258.
[4]R. W. G. Wyckoff, *Crystal Structures*, 2nd ed., Vol. 2 (Wiley Interscience, New York, 1964).
[5]H. P. Beck, J. Solid State Chem. **17**, 275 (1976).
[6]K. Govinda Rajan and A. Jestin Lenus, Pramana **65**, 323 (2005).
[7]H. von Seggern, T. Voigt, W. Knupfeer, and G. Lange, J. Appl. Phys. **64**, 1405 (1998).
[8]M. K. Crawford, L. H. Brixner, and K. Somaiah, J. Appl. Phys. **66**, 3758 (1989).

[9]K. Takahashi, J. Miyahara, and Y. Shibahara, J. Electrochem. Soc. **132**, 1492 (1985).
[10]H. Riesen and W. A. Kaczmarek, Inorg. Chem. **46**, 7235 (2007).
[11]Y. R. Shen, T. Gregorian, and W. B. Holzapfel, High Press. Res. **7**, 73 (1991).
[12]P. Comodi and P. F. Znazzi, J. Appl. Crystallogr. **26**, 843 (1993).
[13]H. P. Beck, A. Limmer, W. Denner, and H. Schulz, Acta Crystallogr. B **38**, 401 (1983).
[14]H. P. Beck, Z. Anorg. Allg. Chem. **459**, 72 (1979).
[15]B. Sundarakkannan, R. Kesavamoorthy, J. A. Nisha, V. Sridharan, and T. Sivakumar, Phys. Rev. B **57**, 11632 (1998).
[16]Y. Dossmann, R. Kuentzler, M. Sieskind, and D. Ayachour, Solid State Commun. **72**, 377 (1989).
[17]K. Somaiah and V. H. Babu, Indian J. Pure Appl. Phys. **14**, 702 (1976).
[18]Y. R. Shen, U. Englisch, L. Chudinovskikh, F. Porsch, R. Haberkon, H. P. Beck, and W. B. Holzapfel, J. Phys. Condens. Matter **6**, 3197 (1994).
[19]N. Subramanian, N. V. Chandrashekar, P. C. Sahu, M. Yousuf, and K. G. Rajan, Phys. Rev. B **58**, R555 (1998).
[20]F. Decremps, M. Fischer, A. Polian, J. P. Itie, and M. Sieskind, Phys. Rev. B **59**, 4011 (1999).
[21]F. Decremps, M. Fischer, A. Polian, and M. Sieskind, Eur. Phys. J. B **5**, 7 (1998).
[22]R. Mittal, S. L. Chaplot, A. Sen, S. N. Achary, and A. K. Tyagi, Phys. Rev. B **67**, 134303 (2003).
[23]G. Kalpana, B. Palanivel, I. B. Shameem Banu, and M. Rajagopalan, Phys. Rev. B **56**, 3532 (1997).
[24]T. Kurobori, Y. Hirose, and M. Takeuchi, Phys. Status Solidi B **220**, R11 (2000).
[25]F. El haj Hassan, H. Akbarzadeh, S. J. Hashemifar, and A. Mokhtari, J. Phys. Chem. Solids **65**, 1871 (2004).
[26]V. D'Anna, L. M. L. Daku, H. Hagemann, and F. Kubel, Phys. Rev. B **82**, 024108 (2010).
[27]M. Laval, M. Mosszynski, R. Allemand, E. Cormoreche, P. Guinet, R. Odru, and J. Vacher, Nucl. Instrum. Methods Phys. Res. **206**, 169 (1983).
[28]C. L. Woody, P. W. Levy, and J. A. Kierstead, IEEE Trans. Nucl. Sci. **36**, 536 (1989).
[29]E. D. Bourret-Courchesne, G. Bizarri, S. M. Hanrahan, G. Gundiah, Z. Yan, and S. E. Derenzo, Nucl. Instrum. Methods Phys. Res. **613**, 95 (2010).
[30]D. J. Singh and L. Nordstrom, *Planewaves, Pseudopotentials, and the LAPW Method*, 2nd ed. (Springer Verlag, Berlin, 2006).
[31]P. Blaha, K. Schwarz, G. Madsen, D. Kvasnicka, and J. Luitz, WIEN2k, An Augmented Plane Wave + Local Orbitals Program for Calculating Crystal Properties (K. Schwarz, Tech. Univ. Wien, Austria, 2001).
[32]D. Singh, Phys. Rev. B **43**, 6388 (1991).
[33]R. Kesavamoorthy, G. V. N. Rao, B. Sundarakkannan, G. Ghosh, and V. S. Sastry, Powder Diffraction **12**, 255 (1997).
[34]H. P. Beck, Z. Anorg. Allg. Chem. **451**, 73 (1979).
[35]B. W. Liebich and D. Nicollin, Acta Crystallogr. B **33**, 2790 (1977).
[36]J. P. Perdew, K. Burke, and M. Ernzerhof, Phys. Rev. Lett. **77**, 3865 (1996).
[37]F. Tran and P. Blaha, Phys. Rev. Lett. **102**, 226401 (2009).
[38]D. J. Singh, Phys. Rev. B **82**, 155145 (2010).
[39]D. J. Singh, Phys. Rev. B **82**, 205102 (2010).
[40]V. Milman, B. Winkler, J. A. White, C. J. Pickard, M. C. Payne, E. V. Akhmatskaya, and R. H. Nobes, Int. J. Quantum Chem. **77**, 895 (2000).
[41]M. D. Segall, P. J. D. Lindan, M. J. Probert, C. J. Pickard, P. J. Hasnip, S. J. Clark, and M. C. Payne, J. Phys. Condens. Matter **14**, 2717 (2002).
[42]D. Vanderbilt, Phys. Rev. B **41**, 7892 (1990).
[43]J. P. Perdew and A. Zunger, Phys. Rev. B **23**, 5048 (1981).
[44]C. Filippi, D. J. Singh, and C. J. Umrigar, Phys. Rev. B **50**, 14947 (1994).
[45]Z. Wu, R. E. Cohen, and D. J. Singh, Phys. Rev. B **70**, 104112 (2004).
[46]A. Janotti, S. H. Wei, and D. J. Singh, Phys. Rev. B **64**, 174107 (2001).
[47]While this is an ionic compound, the structure consists of overall neutral $X\mathrm{BaF_2Ba}X$ blocks as shown. The internal bonding of these blocks is strongly ionic. However, these blocks have the anions on the outside with a rather large interblock separation. Such structures are quite often micalike with dispersion interactions playing an important role in the interblock bonding (Ref. 1), as in $\mathrm{CdI_2}$ structure halides, $\mathrm{CoO_2}$, which can be intercalated with variable amounts of $\mathrm{Na^+}$ or $\mathrm{Li^+}$ ions, of importance in battery technology, and even water, as well as in compounds such as $\mathrm{MoS_2}$, which is also readily intercalated and is used as a lubricant. In any case, these compounds consist of $X\mathrm{BaF_2Ba}X$ blocks that are stabilized by ionic bonds and that interact weakly with each other.
[48]M. J. Mehl, J. E. Osburn, D. A. Papaconstantopoulos, and B. M. Klein, Phys. Rev. B **41**, 10311 (1990).
[49]F. Decremps, M. Fischer, A. Polian, and M. Sieskind, High Temp. High Press. **30**, 235 (1998).
[50]M. Sieskind, A. Pollian, M. Fischer, and F. Decremps, J. Phys. Chem. Solids **59**, 75 (1998).
[51]M. Born and K. Huang, *Dynamical Theory of Crystal Lattices* (Oxford University Press, Oxford, 1998).
[52]R. Hill, Proc. Phys. Soc. London, Sect. A **65**, 349 (1952).
[53]S. F. Pugh, Philos. Mag. **45**, 823 (1954).
[54]D. J. Singh, Appl. Phys. Lett. **92**, 201908 (2008).
[55]A. Lempicki, C. Brecher, H. Lingertat, and V. K. Sarin, US Patent No. 6 967 330 (22 November 2000).
[56]S. R. Podowitz, R. M. Gaume, W. T. Hong, A. Laouar, and R. S. Feigelson, IEEE Trans. Nucl. Sci. **57**, 3827 (2010).